PAPER

Check for updates

GC-FTICR mass spectrometry with dopant assisted atmospheric pressure photoionization: application to the characterization of plastic pyrolysis oil†

Charlotte Mase,[a,b,c] Julien F. Maillard,[b,c] Marco Piparo,[b,c] Lukas Friederici,[d] Christopher P. Rüger,[c,d] Sabrina Marceau,[b,c] Benoit Paupy,[b,c] Marie Hubert-Roux,[a,c] Carlos Afonso [ID] *[a,c] and Pierre Giusti[a,b,c]

Pyrolysis is a promising way to convert plastic waste into valuable resources. However, for downstream upgrading processes, many undesirable species, such as conjugated diolefins or heteroatom-containing compounds, can be generated during this pyrolysis. In-depth chemical characterization is therefore required to improve conversion and valorization. Because of the high molecular diversity found in these samples, advanced analytical instrumentation is needed to provide accurate and complete characterization. Generally, direct infusion Fourier transform mass spectrometry is used to gather information at the molecular level, but it has the disadvantage of limited structural insights. To overcome this drawback, gas chromatography has been coupled to Fourier transform ion cyclotron resonance mass spectrometry. By taking advantage of soft atmospheric pressure photoionization, which preserves molecular information, and the use of different dopants (pyrrole, toluene, and benzene), selective ionization of different chemical families was achieved. Differences in the ionization energy of the dopants will only allow the ionization of the molecules of the pyrolysis oil which have lower ionization energy, or which are accessible *via* specific chemical ionization pathways. With a selective focus on hydrocarbon species and especially hydrocarbon species having a double bond equivalent (DBE) value of 2, pyrrole is prone to better ionize low-mass molecules with lower retention times compared to the dopant benzene, which allowed better ionization of high-mass molecules with higher retention times. The toluene dopant presented the advantage of ionizing both low and high mass molecules.

[a]*Univ Rouen Normandie, INSA Rouen Normandie, CNRS, Normandie Univ, COBRA UMR 6014, INC3M FR 3038, F-76000 Rouen, France.*
E-mail: carlos.afonso@univ-rouen.fr
[b]*TotalEnergies OneTech, Total Research and Technology Gonfreville TRTG, BP 27, 76700 Harfleur, France*
[c]*International Joint Laboratory – iC2MC: Complex Matrices Molecular Characterization, TRTG, BP 27, 76700 Harfleur, France*
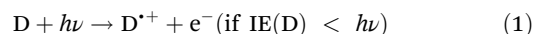[d]*Joint Mass Spectrometry Centre/Chair of Analytical Chemistry, University of Rostock, Albert-Einstein-Straße 27, 18059 Rostock, Germany*
†Electronic supplementary information (ESI) available. See DOI: https://doi.org/10.1039/d3an01246h

1. Introduction

Due to their uncontrolled origin, pyrolysis oils produced from plastic waste materials contain a significant number of undesirable compounds such as heteroatom-containing compounds and conjugated diolefins.[1–4] Among the heteroatom-containing compounds, nitrogen-containing compounds are of particular interest because they are known to poison catalysts in upgrading refining processes. Their characterization is already reported in the literature.[1,5] Concerning the conjugated diolefins, they are known to be largely responsible for oligomerization reactions, deposit, and gumming formation in refinery processes.[6,7] A detailed chemical description of plastic waste-based pyrolysis oil is, therefore, essential to improve the conversion and valorization processes. The chemical composition knowledge of this feedstock will help to improve the pyrolysis reactor parameters. Like petroleum crude oils, plastic pyrolysis oils are complex organic mixtures composed of thousands of chemical species covering a wide range of mass and polarity.[1,3,8] Therefore, these complex mixtures require advanced instrumentation to provide accurate and complete characterization. Ultra-high resolution mass spectrometry (UHR-MS) especially Fourier transform ion cyclotron resonance (FTICR), played a significant role in providing a more accurate understanding of the complexity of organic elemental profiles as described for other matrices.[9–11] However, it is insufficient alone to distinguish isomers or to assign molecular structures, which could be important information, in particular, to improve upgrading processes. That is why coupling fragmentation and separation methods

such as gas chromatography (GC),[12–14] liquid chromatography (LC),[15,16] supercritical fluid chromatography (SFC),[17,18] or ion mobility spectrometry (IMS)[19,20] with UHR-MS have been developed and widely used.

The coupling of GC with FTICR MS allowed, first, to separate isomers, and then, to obtain unique molecular formulas using accurate mass spectrometric measurements.[21] This coupling has been implemented for the first time by Solouki and coworkers.[13,14,22] However, the use of an electron ionization (EI) source is responsible for significant fragmentation, which could be challenging for the characterization of complex mixtures. For that reason, the development of atmospheric pressure ionization (API) sources became very popular for this coupling.[23] Indeed, these sources presented the advantage of preserving the molecular or pseudo-molecular ion by generating lower fragmentation. Among these API sources, atmospheric pressure chemical ionization (APCI) has been the most widely used in the context of FTICR MS coupling. APCI is a nonselective ionization technique applied for complex organic mixtures, especially in petroleum and pyrolysis oil investigation.[24] Barrow *et al.* presented the first GC-APCI-FTICR MS coupling in 2014 to study environmental samples from the Athabasca region of Canada.[25] Since then, several studies were performed on various complex organic mixture applications.[26] The review of Rüger *et al.* summarized the published works in the field of gas chromatography coupled to soft ionization mass spectrometry for the molecular description of energy and fuel matrices.[27] Among the hyphenated GC-FTICR MS methods, Schwemer *et al.* have used this coupling method to characterize the volatile and semi-volatile components in heavy fuel oil, diesel fuel, and corresponding primary combustion engine aerosol extracts.[28] Here, sophisticated automatized routines allowed for the robust removal of ionization artifacts, such as oxygen adducts, and the detection of over 5000 molecular features. Streibel *et al.*[29] have shown that GC-APCI-FTICR MS highlighted the heteroatom-containing compounds such as sulfur and oxygen-containing compounds. The same observation was made by Thomas *et al.*, which compared GC-APCI-FTICR MS with direct infusion (DI) APPI-FTICR MS for the environmental contaminants analysis.[30] Heteroatom-containing classes were in common among both DI and GC but they observed a greater relative intensity with GC-APCI-FTICR MS for several heteroatom-containing compounds classes such as oxygenated compounds. The ability to separate isomers by chromatography enabled characterization of several reactive and hazardous compounds as shown by Barrow *et al.*[25] in a study on soil sands, by Lozano *et al.*[31] for the characterization of softwood bio-oil and its esterified product, or by Zuber *et al.* for the characterization of pyrolysis oil from German brown coal.[12] All these works used extracted ion chromatograms of individual molecular compositions, determining the relationship with the retention time. However, some drawbacks of APCI source are reported in the literature such as, adducts formation and reactivities during ionization processes.[24,32,33] To overcome these disadvantages, atmospheric pressure photoionization (APPI) could be used.[34]

APPI can be used in various applications allowing the ionization of a broad range of compound classes including nonpolar compounds.[35] Its concept was largely and in detail reported in the literature.[36–38] In most cases, dopants have been used in APPI leading to a significant improvement in the ionization efficiency and therefore increase of sensitivity.[39,40] Several dopants were explored in APPI. Most typically found are toluene, acetone, anisole, and chlorobenzene. Numerous other solvents or combinations of solvents have also been studied. In this case, ionization is a two-step process with the photoionization of the dopant (D) (eqn (1)) possible if the ionization energy (IE) of the dopant is lower than the photon energy ($h\nu$) followed by charge exchange with the analyte (M) to produce the molecular ion $M^{\bullet+}$ (eqn (2)) with the condition that IE of the molecule is lower than the IE of the dopant.

$$D + h\nu \rightarrow D^{\bullet+} + e^{-} \, (\text{if IE(D)} \; < \; h\nu) \qquad (1)$$

$$D^{\bullet+} + M \rightarrow D + M^{\bullet+} \, (\text{if IE(M)} \; < \; \text{IE(D)}) \qquad (2)$$

Furthermore, depending on their gas phase properties such as proton affinity (PA) or IE, it has been shown that dopants and solvents influence the reactions taking place in the primary ionization and secondary ionization step and therefore can induce a certain selectivity. Especially, Bruins *et al.* have shown that the use of anisole as a dopant allowed a 100-fold increase in the sensitivity of analytes with low proton affinities in acetonitrile.[41] The same observation was realized by Kauppila *et al.* which showed that the ionization efficiency was 1–2 orders higher with dopant than without in the study of 7 polycyclic aromatic hydrocarbons (PAHs).[40] The authors also proved that the charge exchange was favored for low proton affinity solvents and the proton transfer was enhanced with the addition of protic solvent. This approach can be advantageous for the identification of specific compounds in various organic mixtures.

In this study, a light fraction of plastic pyrolysis oil was analyzed by GC-APPI-FTICR MS in positive ion mode. Three dopants, having different proton affinities and ionization energies, were used in the ionization step to first improve the sensitivity and second to selectively ionize the different classes. The dopants used were pyrrole, toluene, and benzene respectively. These experiments were compared to an experiment without the use of a dopant. Furthermore, a comparison to DI-FTICR MS with APPI source, using toluene as a dopant was also realized.

2. Materials and methods

2.1. Sample and reagents

Plastic pyrolysis oil was produced by fast pyrolysis at 410 °C under inert atmosphere without additives. The oil was converted to a light fraction with distillation. This oil was supplied by TotalEnergies TOTB (TotalEnergies OneTech Belgium). The oil obtained contains 85.5 w% of carbon, 13.7 w% of hydrogen, <0.3 w% of nitrogen, <0.3 w% of sulfur, and 0.36 w% of

oxygen. Toluene, pyrrole, and benzene (analytical LC-MS grade with purity higher than 99.7%) were purchased from Fisher Chemical (Hampton, United States). Classical fossil diesel sample (respecting the NF EN 590) was provided by TotalEnergies. Standards molecule solutions were purchased from a petroleum analyzer Company (PAC) (ref. 20001.643 – PNA in AVTUR Gravimetric Blend). It includes toluene, ethyl-benzene, o-xylene, 2-ethyltoluene, n-propylbenzene, trans-deca-hydronaphtalene, 1,2,4-trimethylbenzene, 1,2,4,5-tetramethyl-benzene, pentamethylbenzene, hexamethylbenzene, naphtha-lene and 2-ethylnaphtalene.

2.2. Direct infusion APPI-FTICR MS

Plastic pyrolysis oil was diluted at 0.2 mg mL^{-1} in toluene for DI-APPI-FTICR MS. For this experiment, a hybrid quadrupole 12 T solariX FTICR mass spectrometer (Bruker Daltonics, Germany) was coupled to an APPI II source (Krypton discharge lamp, 10./10.6 eV). The instrument was operated in positive ion mode. Mass spectra were acquired with a mass range of m/z 93–1000 accumulating 100 scans. The signal was digital-ized with 1 M points giving a transient length of 0.2621 s to mimic the acquisition conditions in GC operation mode. The accumulation time was set to 0.1 s at a flow rate of 600 μL h^{-1} giving a resolution of 150 000 at m/z 200. The experimental conditions were as follows: capillary voltage: 900 V; end plate offset: −500 V; nebulizer pressure: 2 bar; desolvation gas flow: 3 L min^{-1}; dry temperature: 150 °C; time of flight: 0.55 ms; and quadrupole lower cut-off m/z 93. The mass spectrometer was externally calibrated using sodium trifluoroacetate solu-tion before sample analysis. A blank of the solvent was recorded with the same conditions before the analysis of the sample.

2.3. Gas chromatography APPI-FTICR MS

1 μL of the plastic pyrolysis oil was directly injected without dilution in a GC 450 (Bruker Daltonics, Germany) using a split/splitless injector equipped with a 30 m Rxi-5Sil column (0.25 mm × 0.25 μm) from Restek (Clementon, United States). A split ratio of 1 : 300 was used. Helium was the carrier gas with a flow rate of 1 mL min^{-1}. The injector and transfer line temperatures were set at 250 °C. The temperature program was set as follows: 50 °C hold for 5 min, ramping 5 °C min^{-1} up to 300 °C and hold for 10 min. The hybrid quadrupole 12 T solariX FTICR mass spectrometer (Bruker Daltonics, Germany) was equipped with a GC-APCI II ion source (Bruker Daltonics, Germany). The source was modified to allow APPI experiments by removing the corona needle and installing a self-build krypton microwave-induced discharge lamp (10.0/10.6 eV) module titled from the upper inlet (Fig. S1b†). Emission characteristics of this source mimic the DI ionization. Furthermore, a T-piece adapter was added to the nebulizer gas inlet to allow the addition of dopant directly in the effluent elution zone. A picture of the modified system is given in Fig. S1a.† The instrument was operated in positive ion mode over the mass range of m/z 93–1000 with 1 scan accumulated and 95% data profile reduction. The signal was digitalized

with 1 M giving a transient length of 0.2621 s (around 3.8 Hz). The accumulation time was set to 0.1 s resulting in a resolu-tion of 115 000 at m/z 200. To allow for direct comparison, other experimental conditions were kept the same as for the DI-APPI-FTICR MS: capillary voltage: 900 V; end plate offset: −500 V; nebulizer pressure: 2 bar; desolvation gas flow: 3 L min^{-1}; dry temperature: 150 °C; time of flight: 0.55 ms; and quadrupole lower cut-off 93. A flow of 5 μL h^{-1} was used for dopant addition.

2.4. Data processing

Data were processed with DataAnalysis (version 5.1, Bruker Daltonics, Germany). Mass spectra were first internally cali-brated using alkylated series (CH$_2$-units) of known CH com-pounds of the plastic pyrolysis oil covering the entire detected mass range (Table S1†). For the GC analysis, mass spectra with substantial signal were averaged for this purpose. m/z values were further assigned with a signal-to-noise ratio (S/N threshold) greater than six. The molecular formula attribution was carried out with the following constraints: C$_{0–100}$, H$_{0–300}$, O$_{0–4}$, N$_{0–3}$, 0 < H/C < 3, −0.5 < double bond equivalent (DBE) < 30 with up to 0.5 ppm error and considering both even and odd electron ion configurations. The molecular composition of plastic pyrolysis oil in each condition was assigned with a final root-mean-square error inferior to 200 ppb.

The peak assignments were finally exported to PyC2MC viewer[42] and OriginPro 2016 (OriginLab) to visualize the datasets.

The class distribution is represented by bar plots with class relative abundance. A compound class includes all compounds with fixed heteroatom numbers. This graphical representation allows a general view of the chemical composition of a sample.

DBE versus carbon number plots provide information on the aromaticity and the unsaturation of a given molecule. These plots are used to represent a given class such as the CH class allowing identification of the main compounds as a func-tion of their size and their aromaticity. DBE values are calcu-lated with eqn (3) with n_C: number of the carbon atom, n_H: number of the hydrogen atom, and n_N: number of the nitrogen atom.

$$DBE = n_c - \frac{n_H}{2} + \frac{n_N}{2} + 1. \quad (3)$$
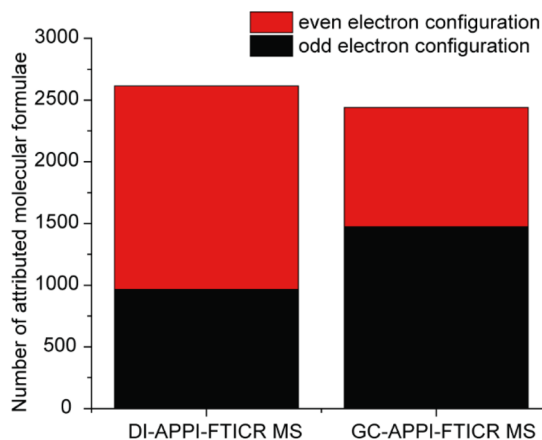
3. Results and discussion

3.1. Comparison between DI-APPI-FTICR MS and GC-APPI-FTICR MS

The light fraction of plastic pyrolysis oil was analyzed by both DI-APPI-FTICR MS and GC-APPI-FTICR MS using toluene as a dopant, which represents the classical workflow used with this kind of ionization source.[8,43,44] Fig. 1a displays the two mass spectra obtained for each experiment. Note that the mass spec-trum of the GC experiment corresponded to the average mass spectra over 0 to 80 min (8650 scans). Each presented an ion
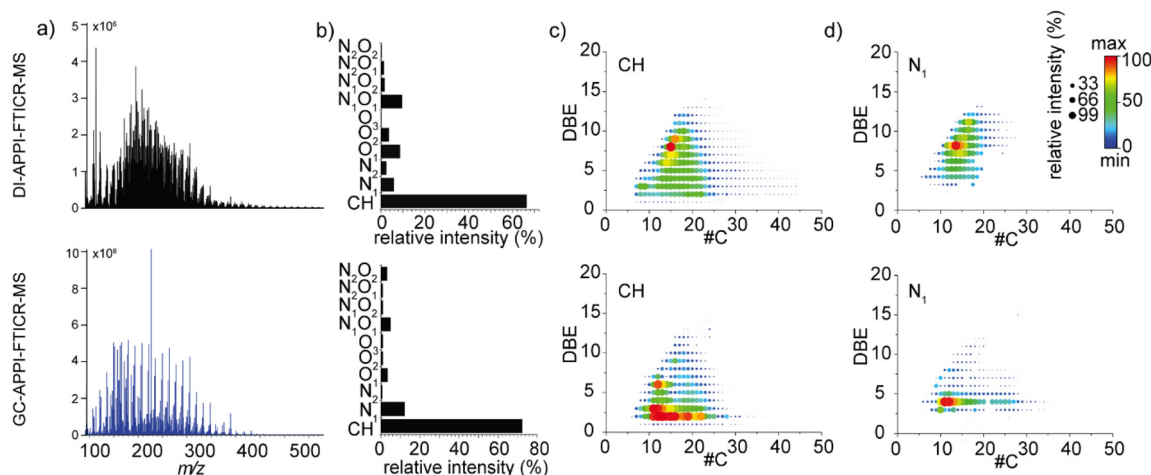
Fig. 1 (a) Mass spectra of plastic pyrolysis oil obtained for DI-APPI-FTICR MS (at the top) and average mass spectra over 0 to 80 min obtained for GC-APPI-FTICR MS with toluene as dopant (at the bottom) with their (b) molecular classes distribution, (c) DBE *versus* carbon number plot of CH class, and (d) DBE *versus* carbon number plot of N_1 class.

distribution composed of thousands of peaks covering a mass range between m/z 100 and m/z 500. A slight bimodal distribution could be observed in the mass spectrum obtained for GC, with two maxima at m/z 150 and m/z 250, whereas a unimodal distribution with a maximum at m/z 200 is obtained in the case of DI. Comparison of DI-APPI-FTICR MS and GC-APPI-FTICR MS spectra (Fig. 1) revealed that GC was more sensitive in detecting low-mass compounds compared to DI. However, a similar number of attributed molecular formula was obtained for both setups with 2615 species identified using DI and 2441 for GC. Interestingly, differences could be found in the electron configuration ions of the assigned species (Fig. 2). Both odd-electron configuration ions ($M^{\bullet+}$) and even-electron configuration ions ($[M + H]^+$) were detected. Mostly odd electron ions were obtained in the case of GC covering 81% of the attributed species whereas a balanced distribution was obtained in the case of DI. Indeed, as already shown by Kauppila *et al.*, the proton transfer reaction occurs

with solvent molecules having a proton affinity higher than the deprotonated dopant radical cation.[40] Consequently, the addition of dopants directly in the ionization step allowed a more effective electron transfer thanks to the separation obtained with GC.[44,45]

As presented in Fig. 1b, for both experiments, the CH class is most abundant. It corresponds to more than 65% of the attributions for the DI and more than 75% for the GC in relative intensity. This result was not surprising, as plastic-based materials and therefore their pyrolysis oils contain mainly hydrocarbon compounds.[2] The remaining signals were recognized as nitrogen- and oxygen-containing species. Especially, more than 10% of N_1 class ions were detected by GC and more than 10% of N_1O_1 class ions were detected by DI. This kind of species was already observed on the heavier plastic pyrolysis oil fraction.[1,46]

The DBE *versus* carbon number plots of the CH and N_1 classes including both odd and even electron configuration ions are shown in Fig. 1c and d respectively. For the CH class, the average DBE and the average carbon number by intensity weighted were respectively 6.5 and 18.8 for DI, and 5.7 and 16.9 for GC. On average higher number of aromatic species was obtained in the case of DI with major compounds presenting DBE values of 8 and 9 that may present naphthalene or diphenyl cores. While GC allowed the ionization of more aliphatic species with intense distribution at the DBE 2 value that may correspond to diolefins, alkyl-naphthenes, or alkynes. The difference in behavior among DI-APPI-FTICR MS and GC-APPI-FTICR MS experiments may be due to ionization discrimination in DI towards aromatic molecules that are expected to have a better ionization efficiency in APPI[36] or due to technical aspect of the GC injection[47] compared to less biased direct infusion.

The DBE *versus* carbon number plots of the CH class separating both odd and even-electron configuration ions were given in Fig. S2.† The separation of both ion configurations

Fig. 2 Number of attributed species for DI-APPI-FTICR MS and GC-APPI-FTICR MS experiments.

allows the highlight of different hydrocarbon series as aromatic species are more likely to yield radical cations. In addition to the aromatic distribution with ions ionized as odd-electron configuration ions, the DI-APPI-FTICR MS allowed the ionization of a fewer aromatic series with DBE values of 3 and 4 that may correspond to triene or cyclopentadiene.[4,8] These species were also observed in GC-APPI-FTICR MS.

For the N_1 class (Fig. 1d), the same observation as the CH class was observed. DI-APPI-FTICR MS allowed the ionization of more aromatic species with an intense distribution of a DBE value of 9 that may correspond to phenanthrene or fluorene, whereas GC-APPI-FTICR MS allowed the ionization of less aromatic species with a DBE value of 4 with benzene aromatic core. Therefore, GC separation allowed having a more focused characterization of plastic pyrolysis oil with enhanced detection of fewer aromatic species (DBE < 4). This can be explained by the phenomenon of competition to the ionization present in DI-APPI-FTICR MS. Indeed, in DI, the aromatic species will preferentially ionize compared to aliphatic species. Thanks to its separation, GC allows aliphatic species to arrive separately from aromatic species at the ionization source and thus ionize with less competition bias. In our case, this means that the aromatic species might be not the main species in the plastic pyrolysis oil and focus can be laid on other relevant compound classes with less unsaturation.

3.2. GC-APPI-FTICR MS with different dopants

3.2.1. Overall description. With APPI, the use of dopants is required to achieve high ionization efficiency.[41,44,45] Reactions leading to ionization of the analyte in APPI involve in this case a two-step process, as presented in eqn (1) and (2). After initial photoionization of the dopant, the ionization of the analyte can occur by charge exchange if the ionization energy of the analyte is below that of the dopant. In addition, the formation of protonated molecules can also occur especially for high proton affinity molecules under the presence of protic solvents. Consequently, dopants can selectively ionize molecular classes.[40,44] Different dopants were used in GC-APPI-FTICR MS experiments to obtain different ionization selectivity. Such comparison was already shown with various dopants in direct infusion, such as toluene and anisole for aromatic standards by Kauppila *et al.*[44] Pyrrole, toluene, and benzene with ionization energy of 8.2 eV, 8.8 eV, and 9.2 eV respectively and proton affinity of respectively 875.4 kJ mol^{-1}, 784.0 kJ mol^{-1}, and 750.4 kJ mol^{-1} (NIST webbook) respectively were used. These three conditions were compared with the experiment without a dopant. Fig. 3a shows the four total ion chromatograms (TIC) for the analysis of the plastic pyrolysis oil with pyrrole, toluene, and benzene as dopants, and without dopants. The first observation is the increase of signal intensity with the presence of a dopant, commonly also reported for direct infusion experiments.[44] The intensity for the experiments with dopants showed an increase by a factor of 500 for pyrrole and toluene and 600 for benzene as dopants compared to the experiment without dopants. As expected, the use of dopants allowed a clear improvement of the signal intensity

and allowed the detection of a larger number of species by substantially increasing the signal-to-noise ratios by a factor of over 10. Fig. 3b presents the respective average mass spectra for the four experiments. It is interesting to note that a broader distribution of ions along the m/z dimension was obtained in the case of toluene and benzene experiments. Fig. 3c presents the compound class distribution obtained by the average mass spectrum over 0 to 80 min.

As for the DI-APPI-FTICR MS approach, the CH class was the most representative with more than 60% in each case. Pyrrole and toluene yielded the detection of relatively abundant N_1 class ions. However, with pyrrole, this class could correspond to pyrrole adduct $[M + C_4H_5N]^{\bullet+}$ produced during the ionization step. Hydrocarbon species and their corresponding pyrrole adduct presented the same extracted ion chromatogram (EIC). The EIC of three ions, $C_7H_{12}^{\bullet+}$, $C_9H_{14}^{\bullet+}$, and $C_{11}H_{16}^{\bullet+}$, and their corresponding pyrrole adducts were given in Fig. S3.† The chromatograms are perfectly aligned in retention time although one can note differences in relative abundance depending on the isomer. The same observation was made during the analysis of aromatic standard molecules that yielded both $M^{\bullet+}$ and $[M + C_4H_5N]^{\bullet+}$ ions with pyrrole as a dopant whereas only the $M^{\bullet+}$ was obtained with toluene as a dopant (Fig. S4†). Consequently, depending on the dopant, it can be observed the induction of chemical ionization pathways, triggering another level of structural dependency accessible *via* gas chromatographic hyphenation.

Although the CH class is the most abundant in each case, the number of molecular formulas assigned varies according to the dopant used (Fig. 3c). Comparing the three dopants, we found that the number of ionized species significantly increased with the ionization energy of the dopant. This is consistent with the widest distribution obtained with the benzene dopant compared to the other dopants. We can see that more than 100 additional species were assigned with dopants in comparison with the no dopant condition nevertheless presented the most abundant relative intensity in the CH class (more than 90%). Benzene allowed the ionization of more compounds with 370 attributed molecular formulas. Thus, we can conclude the higher the ionization energy of the dopant, the higher the exhaustivity as already proven by the analysis of standards by DI-APPI-MS.[40] Note that the isomeric diversity allowed by the GC dimension was not considered as each molecular formula corresponds to many structural formulas as seen in Fig. S3.†

The corresponding two-dimensional (2D) m/z *versus* retention time plots are given in Fig. 3d. This representation allowed us to identify three distinct areas. The two first ones (areas 1 and 2) correspond to intact species ($[M + H]^+$ and $M^{\bullet+}$ ions). In agreement with gas chromatography elution theory, the m/z proportionally increased with retention time. The mass spectra of both areas were extracted to identify the molecular nature of the species (example for benzene is given in Fig. S5†). The distribution (area 1) with a positive m/z offset (higher m/z values for the same retention times) corresponded to nitrogen-containing species such as N_1 and $N_{1-2}O_{1-2}$ and
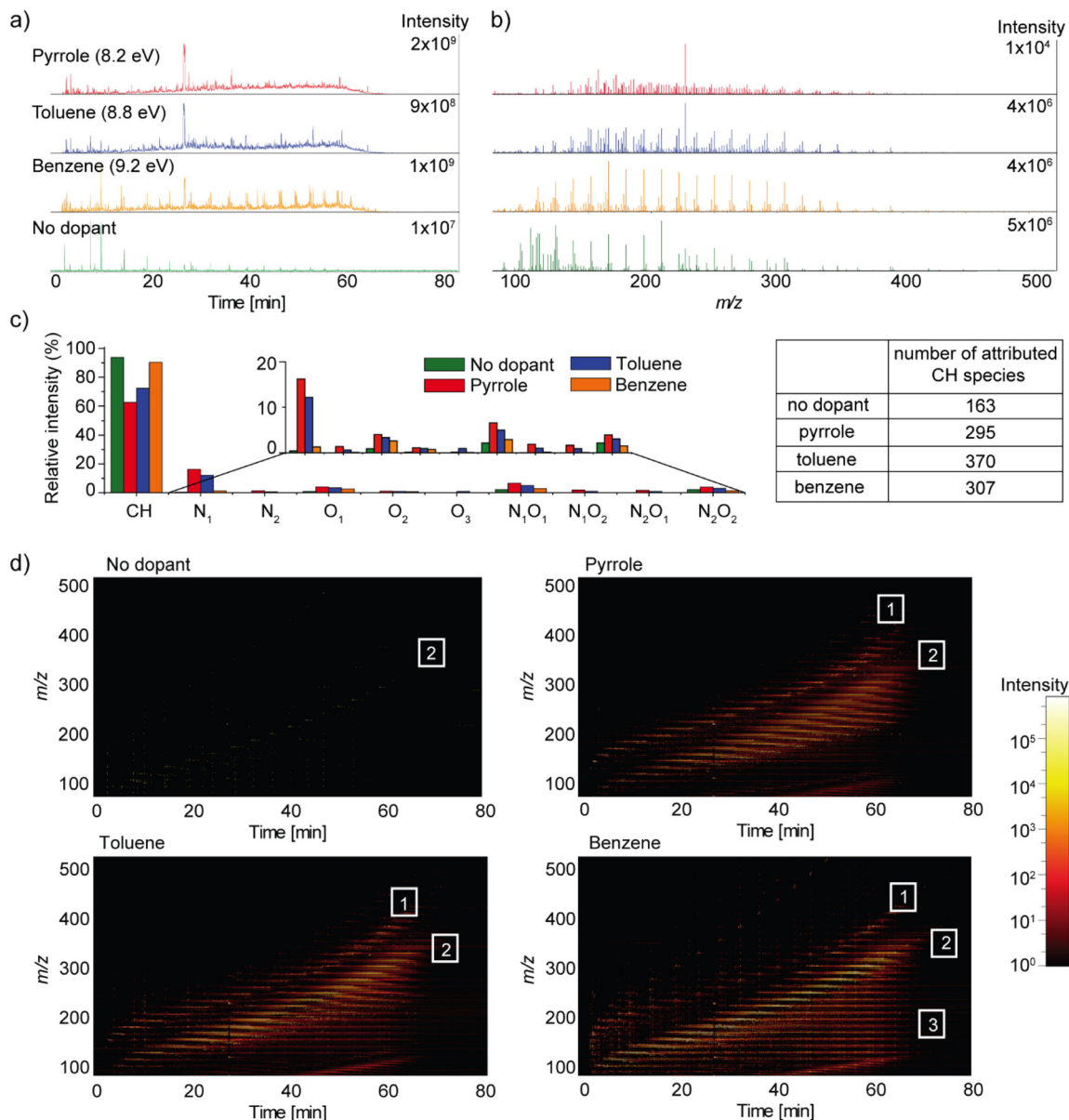
Fig. 3 (a) Total ion chromatograms (TIC) of plastic pyrolysis oil obtained by GC-APPI-FTICR MS with pyrrole (in red), toluene (in blue), benzene (in yellow), and without dopant (in green). (b) Corresponding average mass spectra. (c) Compound class distribution by the average mass spectrum over 0 to 80 min with the number of ionized CH species. (d) Two-dimensional plots representing m/z in the function of retention time (first area corresponding to intact nitrogen-containing compounds, second area to intact hydrocarbon compounds, and third to dealkylation fragments).

the dominating distribution (area 2) to CH compounds. The first area is more apparent when using pyrrole and toluene as dopants as previously discussed. A main additional area was additionally observed in the case of the experiment with benzene as a dopant (area 3). This area present dealkylation fragment as they are low mass ions which are observed at higher retention time. The fragmentation species were evidenced on the 2D-maps by vertical lines from the intact molecules identified in both areas 1 and 2, reflecting retention indexes too high for the given elution retention time compared to natural mixture estimations, particularly when considering chemical information, such as DBE, accessible *via* the sum for-

mulae attribution.[48] The benzene dopant generated a wider number of peaks corresponding to the fragmentation of high-mass molecules compared to the experiment without the dopant and with the pyrrole dopant. This can be explained by the higher ionization energy of the benzene which leads to a higher transfer energy to the molecules inducing fragmentation. The GC is essential here to identify these fragments and the *N*-adducts formation and therefore correct them. Indeed, with direct infusion, it could easily be overlooked and leading to errors in data interpretation. A small portion of fragmentation was also observed in the case of toluene dopants mainly on high-mass compounds, but the fragmentation was substan-

tially less intense. Less fragments were observed for the pyrrole experiment (around 130 attributed molecular formula, against around 1300 for benzene and 1000 for toluene). We can conclude that the higher the ionization energy of the dopant, the more fragmentations are present even though the ionization efficiency is better.[44] The choice of dopant was therefore important according to the desired information. This observation was confirmed by the analysis of aromatic hydrocarbon standards where the fragmentation of compounds increased with the ionization energy of the dopant. The chromatogram and two examples of fragmentation are shown in Fig. S6.† The presence of these fragmentations provided structural information without the total loss of the precursor ions, which can only be achieved by prior GC separation.

These produced fragments can be removed after molecular attribution and further processing applying dedicated algorithms published for GC-APCI MS and adapted towards the dominant dealkylation observed in the study of Schwemer *et al.*[48] and Rüger *et al.*[49] The two first areas corresponding respectively to nitrogen-containing compounds and hydrocarbon compounds were therefore selected and extracted using DataAnalysis™ to avoid the presence of fragmentation products. The DBE *versus* carbon number plots of both CH and N_1 classes were given in Fig. 4a and b respectively. As expected, the use of a dopant allowed a more in-depth description of the sample. For CH class, ion distributions showing both aromatic (DBE $\geq$ 4) and aliphatic (DBE < 4) species were observed with pyrrole, toluene, and benzene dopants whereas only aliphatic species were detected without dopants. The aromatic distribution was however less intense with benzene dopant. Concerning low DBE species, toluene and benzene yielded the largest coverage with carbon atom numbers up to 40 for the toluene and 35 for benzene. Especially, both conditions provided significant information on DBE 2 species. From an industrial point of view, the identification and charac-

terization of these species is of particular interest. Indeed, among them, conjugated diolefins were problematic because they are responsible for gum formation or polymerization during refining processes.[6] The DBE *versus* carbon number plots using fold change as a color map is given in Fig. S7.† They emphasize similarities and differences in the common chemical space based on intensity/abundance. Comparison between no dopant *vs.* pyrrole experiment, no dopant *vs.* toluene, no dopant *vs.* benzene, pyrrole *vs.* benzene, pyrrole *vs.* toluene, and toluene *vs.* benzene are given. On the other hand, pyrrole allowed a better ionization of aromatic species whereas toluene and benzene presented a higher intensity for the species with lower DBE values. As previously mentioned, the N_1 class was also well ionized with toluene and pyrrole as dopants the latter case they correspond in part to pyrrole adducts. The DBE *versus* carbon number plots of this class is given in Fig. 4d. This class is not observed without dopant as it is less abundant and falls below the detection limit. For the experiment with a dopant, the trend is opposite to the trend observed for the CH class. Pyrrole and toluene as dopants allowed the ionization of low DBE species whereas benzene allowed the ionization of higher DBE species corresponding mainly to aromatic molecules. The distribution was however narrower with the benzene that present a main distribution with carbon number between 8 and 20 against 8 to 40 for the pyrrole and the toluene. The DBE *versus* carbon number plots using fold change as a color map are given in Fig. S8.†

The contribution of the dopant was also evaluated in direct infusion (Fig. S9†) yielding the same observation as with the GC coupling. The intensity increases with the ionization energy of the dopant. The number of CH molecules was similar for the experiments with toluene and benzene as dopant and lower for the experiment with pyrrole as dopant. In each case, the number was significantly lower compared to the number of CH molecules obtained in GC. The use of GC is

Fig. 4 DBE *versus* carbon number plots for (a) CH class and (b) N_1 class corresponding respectively to areas 2 and 1 of the 2D maps.

therefore required to have a better characterization. Finally, as observed in GC experiments, pyrrole tends to ionize better aromatic molecules (DBE ≥ 4).

3.2.2. In-depth study on hydrocarbon species

3.2.2.1. GC retention times for the visualization of the DBE versus carbon number plots. To highlight the selectivity of the dopants, the next part will be focused on the hydrocarbon class. For that, compounds of area 2 in Fig. 3d were exported to avoid the presence of fragments and some adducts. The chromatogram was then sliced into seven equal-width time segments. Mass spectra were exported for each segment corresponding to an average of 10 min representing a balance

between useful chromatographic information and the quality of the mass spectra as done in the work of Barrow *et al.*[25] (Fig. S10–S13†). Future work will focus on utilizing the full chromatographic information,[50] but here discussion on the complex emerging matrix of plastic pyrolysis oils is simplified. At lower retention times, a limited number of lower-mass compounds predominate. With increased retention time, heavier components become more prevalent with overall higher spectral complexity. The DBE *versus* carbon number plots of the CH class of these average mass spectra as a function of retention time, is shown in Fig. 5. We can see the increase of carbon atom numbers with the analysis time as excepted and

Fig. 5 DBE *versus* carbon number plots of CH class for plastic pyrolysis oil for seven retention time segments of GC-APPI-FTICR MS experiments with (a) pyrrole (red), (b) toluene (blue), (c) benzene (yellow), and (d) no dopant (green) for the CH class. The relative intensity was normalized for each DBE *versus* the carbon number plot.

already observed by Barrow *et al.* investigating Athabasca oil sands.[25] As observed in the broadband DBE *versus* carbon number plots in Fig. 4a, the intensity of aromatic species was higher with pyrrole as a dopant whereas the intensity of the aliphatic species was higher with toluene and benzene as dopants in agreement with the ionization energy of these chemical classes (IE(aromatics) < IE(aliphatics)). Among aromatic species, high DBE molecules were detected at higher retention times for a similar carbon atom number. Compared to the broadband, high-DBE values molecules as observed in the sixth and seventh segments (50–60 min and 60–70 min) of pyrrole were described. Among aliphatic species, species with

DBE value of 3 were the most abundant with toluene as a dopant. Species with a DBE value of 2 observed with toluene presented a higher carbon atom number between 15 and 25 compared to species with DBE value of 3. A similar relative intensity between species with DBE values of 2 and 3 was observed with benzene as a dopant. Compared to toluene, benzene allowed the ionization of species with DBE value of 2 covering a large carbon atom number range between 5 and 25.

3.2.2.2. Effect of the dopant on the DBE 2 species. In this section, attention was focused on the hydrocarbon species presenting DBE value of 2. Indeed, these species present high industrial interest because they encompass reactive species such as diolefins or alkynes, which are largely responsible for oligomerization reactions, deposit, and gumming formation in refinery processes. For this reason, 25 species of the CH class with DBE value of 2 were extracted. The list of species and corresponding extracted ion chromatograms (EIC) are given in Table S2.† Fig. 6 shows the EIC of these species obtained with a precision of around 1 mDa at the selected *m/z* value. As previously observed, the elution time of CH compounds is proportional to the number of carbon atoms. Only low-mass CH molecules were detected in the experiment without a dopant while all selected molecules covering *m/z* from 120 to 460 were detected only using dopants. In particular, in Fig. 6a it has been observed that using pyrrole as a dopant low-mass molecules were better ionized. Using toluene uniform ionization has been observed along the whole chromatogram. On the contrary, using benzene higher molecular mass compounds were more efficiently ionized.

4. Conclusion

The hyphenation of GC and FTICR MS applying soft atmospheric pressure photoionization with dopants was for the first time shown in the presented work. This ionization source overcomes the disadvantages of artifacts that can be obtained with APCI or the high selectivity to a narrow chemical space by APLI classically presented.[51] Moreover, the use of different dopants in the ionization step allowed us to ionize selectively molecular classes according to their ionization energies. The application to a plastic pyrolysis oil evidenced a certain structural and mass selectivity during the ionization. Pyrrole tended to better ionize aromatic species (DBE > 4) and low-mass molecules with lower retention times compared to benzene, which allowed better ionization of species with lower DBE values (DBE < 4) and high-mass molecules with higher retention times. The toluene presented the advantage of ionizing both aliphatic and aromatic species observed with pyrrole and benzene and with low and high masses. To conclude, this work can be adapted to other complex organic mixtures. The choice of dopants must be made according to the desired molecular information. Other dopants or even mixtures of dopants can be considered to obtain global information about the sample. This technique will allow for complementary information compared to direct infusion attempts. Particularly for

Fig. 6 Extracted ion chromatograms (EIC) of CH species with DBE value of 2 in ascending order for plastic pyrolysis oil with (a) pyrrole, (b) toluene, (c) benzene, and (d) no dopant. The EIC was obtained with a precision of around 1 mDa on the selected 100–500 *m/z* value.

the applications towards emerging matrices from energy transition and recycling such as the herein investigated plastic pyrolysis oil, the potential of this technique is highlighted. Thus, future work will focus on using tandem mass spectrometry to elucidate the molecular structures of the sample constituents, which may provide information about the dopant ionization mechanism.

Conflicts of interest

There are no conflicts to declare.

Acknowledgements

References

1 C. Mase, J. F. Maillard, B. Paupy, M. Farenc, C. Adam, M. Hubert-Roux, C. Afonso and P. Giusti, Molecular Characterization of a Mixed Plastic Pyrolysis Oil from Municipal Wastes by Direct Infusion Fourier Transform Ion Cyclotron Resonance Mass Spectrometry, *Energy Fuels*, 2021, **35**(18), 14828–14837.

2 S. D. Anuar Sharuddin, F. Abnisa, W. M. A. Wan Daud and M. K. Aroua, A review on pyrolysis of plastic wastes, *Energy Convers. Manage.*, 2016, **115**, 308–326.

3 A. Dhahak, V. Carre, F. Aubriet, G. Mauviel and V. Burkle-Vitzthum, Analysis of Products Obtained from Slow Pyrolysis of Poly(ethylene terephthalate) by Fourier Transform Ion Cyclotron Resonance Mass Spectrometry Coupled to Electrospray Ionization (ESI) and Laser Desorption Ionization (LDI), *Ind. Eng. Chem. Res.*, 2020, **59**(4), 1495–1504.

4 R. L. Ware, S. M. Rowland, J. Lu, R. P. Rodgers and A. G. Marshall, Compositional and Structural Analysis of Silica Gel Fractions from Municipal Waste Pyrolysis Oils, *Energy Fuels*, 2018, **32**(7), 7752–7761.

5 C. Mase, J. F. Maillard, B. Paupy, M. Hubert-Roux, C. Afonso and P. Giusti, Speciation and Semiquantification of Nitrogen-Containing Species in Complex Mixtures: Application to Plastic Pyrolysis Oil, *ACS Omega*, 2022, **7**(23), 19428–19436.

6 D. F. de Andrade, D. R. Fernandes and J. L. Miranda, Methods for the determination of conjugated dienes in petroleum products: A review, *Fuel*, 2010, **89**(8), 1796–1805.

7 K. E. Edwards, K. Qian, F. C. Wang and M. Siskin, Quantitative Analysis of Conjugated Dienes in Hydrocarbon Feeds and Products, *Energy Fuels*, 2005, **19**(5), 2034–2040.

8 R. L. Ware, S. M. Rowland, R. P. Rodgers and A. G. Marshall, Advanced Chemical Characterization of Pyrolysis Oils from Landfill Waste, Recycled Plastics, and Forestry Residue, *Energy Fuels*, 2017, **31**(8), 8210–8216.

9 J. Hertzog, C. Mase, M. Hubert-Roux, C. Afonso, P. Giusti and C. Barrère-Mangote, Characterization of Heavy Products from Lignocellulosic Biomass Pyrolysis by Chromatography and Fourier Transform Mass Spectrometry: A Review, *Energy Fuels*, 2021, **35**(22), 17979–18007.

10 J. Maillard, N. Carrasco, I. Schmitz-Afonso, T. Gautier and C. Afonso, Comparison of soluble and insoluble organic matter in analogues of Titan's aerosols, *Earth Planet. Sci. Lett.*, 2018, **495**, 185–191.

11 C. Castilla, C. P. Ruger, S. Marcotte, H. Lavanant and C. Afonso, Direct Inlet Probe Atmospheric Pressure Photo and Chemical Ionization Coupled to Ultrahigh Resolution Mass Spectrometry for the Description of Lignocellulosic Biomass, *J. Am. Soc. Mass Spectrom.*, 2020, **31**(4), 822–831.

12 J. Zuber, M. M. Kroll, P. Rathsack and M. Otto, Gas Chromatography/atmospheric pressure chemical ionization-fourier transform ion cyclotron resonance mass spectrometry of pyrolysis oil from german brown coal, *Int. J. Anal. Chem.*, 2016, **2016**, 5960916.

13 J. Szulejko and T. Solouki, Potential analytical applications of interfacing a GC to an FT-ICR MS: Fingerprinting complex sample matrixes, *Anal. Chem.*, 2002, **74**(14), 3434–3442.

14 Z. Luo, C. Heffner and T. Solouki, Multidimensional GC-fourier transform ion cyclotron resonance MS analyses: Utilizing gas-phase basicities to characterize multicomponent gasoline samples, *J. Chromatogr. Sci.*, 2009, **47**(1), 75–82.

15 W. Schrader and H.-W. J. A. Klein, Liquid chromatography/Fourier transform ion cyclotron resonance mass spectrometry (LC-FTICR MS): an early overview, *Anal. Bioanal. Chem.*, 2004, **379**(7), 1013–1024.

16 C. Reymond, A. Le Masle, C. Colas and N. Charon, A rational strategy based on experimental designs to optimize parameters of a liquid chromatography-mass spectrometry analysis of complex matrices, *Talanta*, 2019, **205**, 120063.

17 C. Reymond, A. Le Masle, C. Colas and N. Charon, Input of an Off-Line, Comprehensive, Three-Dimensional Method (CPCxSFC/HRMS) to Quantify Polycyclic Aromatic Hydrocarbons in Vacuum Gas Oils, *Anal. Chem.*, 2020, **92**(9), 6684–6692.

18 C. Reymond, A. Le Masle, C. Colas and N. Charon, A three-dimensional semi-quantitative method to monitor the evolution of polycyclic aromatic hydrocarbons from vacuum gas oil feedstocks to lighter products, *Fuel*, 2021, **296**, 120175.

19 A. Gaspar, E. V. Kunenkov, R. Lock, M. Desor, I. Perminova and P. Schmitt–Kopplin, Combined utilization of ion mobi-

lity and ultra–high–resolution mass spectrometry to identify multiply charged constituents in natural organic matter, *Rapid Commun. Mass Spectrom.*, 2009, **23**(5), 683–688.

20 J. F. Maillard, J. Le Maître, C. P. Rüger, M. Ridgeway, C. J. Thompson, B. Paupy, M. Hubert-Roux, M. Park, C. Afonso and P. Giusti, Structural analysis of petroporphyrins from asphaltene by trapped ion mobility coupled with Fourier transform ion cyclotron resonance mass spectrometry, *Analyst*, 2021, **146**(13), 4161–4171.

21 Y. Niu, J. Liu, R. Yang, J. Zhang and B. Shao, Atmospheric pressure chemical ionization source as an advantageous technique for gas chromatography-tandem mass spectrometry, *TrAC, Trends Anal. Chem.*, 2020, **132**, 116053.

22 C. Heffner, I. Silwal, J. M. Peckenham and T. Solouki, Emerging Technologies for Identification of Disinfection Byproducts: GC/FT– ICR MS Characterization of Solvent Artifacts, *Environ. Sci. Technol.*, 2007, **41**(15), 5419–5425.

23 J. F. Ayala-Cabrera, L. Montero, S. W. Meckelmann, F. Uteschil and O. J. Schmitz, Review on atmospheric pressure ionization sources for gas chromatography-mass spectrometry. Part I: Current ion source developments and improvements in ionization strategies, *Anal. Chim. Acta*, 2022, **1238**, 340353.

24 C. P. Ruger, T. Miersch, T. Schwemer, M. Sklorz and R. Zimmermann, Hyphenation of Thermal Analysis to Ultrahigh-Resolution Mass Spectrometry (Fourier Transform Ion Cyclotron Resonance Mass Spectrometry) Using Atmospheric Pressure Chemical Ionization For Studying Composition and Thermal Degradation of Complex Materials, *Anal. Chem.*, 2015, **87**(13), 6493–6499.

25 M. P. Barrow, K. M. Peru and J. V. Headley, An added dimension: GC atmospheric pressure chemical ionization FTICR MS and the Athabasca oil sands, *Anal. Chem.*, 2014, **86**(16), 8281–8288.

26 D. Zacs, I. Perkons and V. Bartkevics, Evaluation of analytical performance of gas chromatography coupled with atmospheric pressure chemical ionization Fourier transform ion cyclotron resonance mass spectrometry (GC-APCI-FT-ICR-MS) in the target and non-targeted analysis of brominated and chlorinated flame retardants in food, *Chemosphere*, 2019, **225**, 368–377.

27 C. P. Rüger, O. Tiemann, A. Neumann, T. Streibel and R. J. E. Zimmermann, Fuels, Review on evolved gas analysis mass spectrometry with soft photoionization for the chemical description of petroleum, petroleum-derived materials, and alternative feedstocks, *Energy Fuels*, 2021, **35**(22), 18308–18332.

28 T. Schwemer, C. P. Rüger, M. Sklorz and R. Zimmermann, Gas chromatography coupled to atmospheric pressure chemical ionization FT-ICR mass spectrometry for improvement of data reliability, *Anal. Chem.*, 2015, **87**(24), 11957–11961.

29 T. Streibel, J. Schnelle-Kreis, H. Czech, H. Harndorf, G. Jakobi, J. Jokiniemi, E. Karg, J. Lintelmann, G. Matuschek, B. Michalke, L. Muller, J. Orasche, J. Passig, C. Radischat, R. Rabe, A. Reda, C. Ruger, T. Schwemer,

O. Sippula, B. Stengel, M. Sklorz, T. Torvela, B. Weggler and R. Zimmermann, Aerosol emissions of a ship diesel engine operated with diesel fuel or heavy fuel oil, *Environ. Sci. Pollut. Res. Int.*, 2017, **24**(12), 10976–10991.

30 M. J. Thomas, E. Collinge, M. Witt, D. C. P. Lozano, C. H. Vane, V. Moss-Hayes and M. P. Barrow, Petroleomic depth profiling of Staten Island salt marsh soil: 2ω detection FTICR MS offers a new solution for the analysis of environmental contaminants, *Sci. Total Environ.*, 2019, **662**, 852–862.

31 D. C. P. Lozano, H. E. Jones, R. Gavard, M. J. Thomas, C. X. Ramírez, C. A. Wootton, J. A. S. Chaparro, P. B. O'Connor, S. E. Spencer and D. Rossell, Revealing the Reactivity of Individual Chemical Entities in Complex Mixtures: the Chemistry Behind Bio-Oil Upgrading, *Anal. Chem.*, 2022, **94**(21), 7536–7544.

32 G. Li, X. Li, Z. Ouyang and R. G. Cooks, Carbon-carbon bond activation in saturated hydrocarbons by field-assisted nitrogen fixation, *Angew. Chem., Int. Ed.*, 2013, **52**(3), 1040–1043.

33 C. Wu, K. Qian, C. C. Walters and A. Mennito, Application of atmospheric pressure ionization techniques and tandem mass spectrometry for the characterization of petroleum components, *Int. J. Mass Spectrom.*, 2015, **377**, 728–735.

34 A. Neumann, O. Tiemann, H. J. Hansen, C. P. Ruger and R. Zimmermann, Detailed Comparison of Xenon APPI (9.6/8.4 eV), Krypton APPI (10.6/10.0 eV), APCI, and APLI (266 nm) for Gas Chromatography High Resolution Mass Spectrometry of Standards and Complex Mixtures, *J. Am. Soc. Mass Spectrom.*, 2023, **34**(8), 1632–1646.

35 T. J. Kauppila, J. A. Syage and T. Benter, Recent developments in atmospheric pressure photoionization-mass spectrometry, *Mass Spectrom. Rev.*, 2017, **36**(3), 423–449.

36 A. Raffaelli and A. Saba, Atmospheric pressure photoionization mass spectrometry, *Mass Spectrom. Rev.*, 2003, **22**(5), 318–331.

37 S. J. Bos, S. M. van Leeuwen and U. J. A. Karst, From fundamentals to applications: recent developments in atmospheric pressure photoionization mass spectrometry, *Anal. Bioanal. Chem.*, 2006, **384**, 85–99.

38 S.-S. Cai, L. Short and J. A. Syage, Atmospheric pressure photoionization—The second source for LC-MS?, *LCGC North Am.*, 2008, **26**(3), 286.

39 J. P. Rauha, H. Vuorela and R. Kostiainen, Effect of eluent on the ionization efficiency of flavonoids by ion spray, atmospheric pressure chemical ionization, and atmospheric pressure photoionization mass spectrometry, *J. Mass Spectrom.*, 2001, **36**(12), 1269–1280.

40 T. J. Kauppila, T. Kuuranne, E. C. Meurer, M. N. Eberlin, T. Kotiaho and R. Kostiainen, Atmospheric pressure photoionization mass spectrometry. Ionization mechanism and the effect of solvent on the ionization of naphthalenes, *Anal. Chem.*, 2002, **74**(21), 5470–5479.

41 T. J. Kauppila, R. Kostiainen and A. P. Bruins, Anisole, a new dopant for atmospheric pressure photoionization mass spectrometry of low proton affinity, low ionization

energy compounds, *Rapid Commun. Mass Spectrom.*, 2004, **18**(7), 808–815.

42 M. Sueur, J. F. Maillard, O. Lacroix-Andrivet, C. P. Rüger, P. Giusti, H. Lavanant and C. Afonso, PyC2MC: an open-source software solution for visualization and treatment of high-resolution mass spectrometry data, *J. Am. Soc. Mass Spectrom.*, 2022, **34**(4), 617–626.

43 J. M. Purcell, C. L. Hendrickson, R. P. Rodgers and A. G. Marshall, Atmospheric pressure photoionization proton transfer for complex organic mixtures investigated by fourier transform ion cyclotron resonance mass spectrometry, *J. Am. Soc. Mass Spectrom.*, 2007, **18**(9), 1682–1689.

44 T. J. Kauppila, H. Kersten and T. Benter, The ionization mechanisms in direct and dopant-assisted atmospheric pressure photoionization and atmospheric pressure laser ionization, *J. Am. Soc. Mass Spectrom.*, 2014, **25**(11), 1870–1881.

45 T. J. Kauppila, H. Kersten and T. Benter, Ionization of EPA contaminants in direct and dopant-assisted atmospheric pressure photoionization and atmospheric pressure laser ionization, *J. Am. Soc. Mass Spectrom.*, 2015, **26**(6), 1036–1045.

46 H. E. Toraman, T. Dijkmans, M. R. Djokic, K. M. Van Geem and G. B. Marin, Detailed compositional characterization of plastic waste pyrolysis oil by comprehensive two-dimensional gas-chromatography coupled to multiple detectors, *J. Chromatogr. A*, 2014, **1359**, 237–246.

47 K. Grob, *Split and splitless injection for quantitative gas chromatography: concepts, processes, practical guidelines, sources of error*, John Wiley & Sons, 2008.

48 T. Schwemer, C. P. Ruger, M. Sklorz and R. Zimmermann, Gas Chromatography Coupled to Atmospheric Pressure Chemical Ionization FT-ICR Mass Spectrometry for Improvement of Data Reliability, *Anal. Chem.*, 2015, **87**(24), 11957–11961.

49 C. P. Rüger, T. Schwemer, M. Sklorz, P. B. O'Connor, M. P. Barrow and R. Zimmermann, Comprehensive chemical comparison of fuel composition and aerosol particles emitted from a ship diesel engine by gas chromatography atmospheric pressure chemical ionisation ultra-high resolution mass spectrometry with improved data processing routines, *Eur. J. Mass Spectrom.*, 2017, **23**(1), 28–39.

50 C. P. Rüger, T. Schwemer, M. Sklorz, P. B. O'Connor, M. P. Barrow and R. Zimmermann, Comprehensive chemical comparison of fuel composition and aerosol particles emitted from a ship diesel engine by gas chromatography atmospheric pressure chemical ionisation ultra-high resolution mass spectrometry with improved data processing routines, *Eur. J. Mass Spectrom.*, 2017, **23**(1), 28–39.

51 C. P. Rüger, A. Neumann, M. Sklorz and R. Zimmermann, Atmospheric pressure single photon laser ionization (APSPLI) mass spectrometry using a 157 nm fluorine excimer laser for sensitive and selective detection of non-to semipolar hydrocarbons, *Anal. Chem.*, 2021, **93**(8), 3691–3697.